Live imaging of bidirectional traffic from the ERGIC

Houchaima Ben-Tekaya[1], Kota Miura[2], Rainer Pepperkok[2] and Hans-Peter Hauri[1,*]

[1]Department of Pharmacology and Neurobiology, Biozentrum, University of Basel, Klingelbergstrasse 70, 4056 Basel, Switzerland
[2]Department of Cell Biology and Biophysics, European Molecular Biology Laboratory Heidelberg, 69117 Heidelberg, Germany
*Author for correspondence (e-mail: hans-peter.hauri@unibas.ch)

Accepted 27 October 2004
Journal of Cell Science 118, 357-367 Published by The Company of Biologists 2005
doi:10.1242/jcs.01615

Summary

The endoplasmic reticulum-Golgi intermediate compartment (ERGIC) defined by the cycling lectin ERGIC-53 consists of tubulovesicular clusters, but it is unknown if these membranes are transport vehicles or stationary entities. Here, we show by live imaging that GFP-ERGIC-53 mainly localizes to long-lived stationary and some short-lived highly mobile elements. Unlike the anterograde marker VSV-G-GFP, GFP-ERGIC-53 does not vectorially move to the Golgi upon exit from the ERGIC, as assessed by a novel quantitative vector field method. Dual-color imaging of GFP-ERGIC-53 and a secretory protein (signal-sequence-tagged dsRed) reveals that the stationary elements are sites of repeated sorting of retrograde and anterograde cargo, and are interconnected by highly mobile elements. These results suggest that the ERGIC is stationary and not simply a collection of mobile carriers that mediate protein traffic from endoplasmic reticulum to Golgi.

Supplementary material available online at
http://jcs.biologists.org/cgi/content/full/118/2/357/DC1

Key words: ERGIC-53, Live cell imaging, Membrane traffic, Secretory pathway, Vesicular stomatitis virus G protein

Introduction

Newly synthesized secretory proteins, also termed cargo, leave the endoplasmic reticulum (ER) in COPII-coated vesicles at the part rough-part smooth transitional elements of the ER (Palade, 1975; Bannykh et al., 1996; Schekman and Orci, 1996). These ER-exit sites (ERES) are localized both in the proximity of the Golgi apparatus and more peripherally in the cell. Two major hypotheses explain how cargo is transported from ER to Golgi in higher eukaryotic cells (Farquhar, 1985; Pelham, 1989; Bannykh and Balch, 1997; Glick and Malhotra, 1998; Lippincott-Schwartz et al., 2000; Stephens and Pepperkok, 2001; Beznoussenko and Mironov, 2002; Storrie and Nilsson, 2002). According to the stable compartment model, cargo is packaged into COP II vesicles that fuse with pre-existing tubulovesicular membrane clusters of the ER-Golgi intermediate compartment (ERGIC). Transport vesicles subsequently bud from the ERGIC and fuse with the cis-Golgi. According to the now prevailing maturation model, COP II vesicles fuse with one another to form the ERGIC. The ERGIC clusters then move as mobile transport complexes to the Golgi and form a new cis-cisterna by homotypic fusion.

The ERGIC (Hauri et al., 2000) consists of a constant average number of tubulovesicular clusters that stain positive for the type I membrane lectin ERGIC-53 and the COPI subunit β-COP (Schweizer et al., 1988; Bannykh et al., 1996; Klumperman et al., 1998). It is equivalent to the site at which ER-Golgi transport of the anterograde marker membrane protein VSV-G and some other secretory proteins is blocked at 15°C (Schweizer et al., 1990; Lotti et al., 1992; Blum et al., 2000). Morphological and biochemical data indicate that ERGIC-53 recycles from ERGIC to ER (Lippincott-Schwartz et al., 1990; Aridor et al., 1995; Tang et al., 1995; Kappeler et al., 1997) by a route that appears to largely bypass the Golgi apparatus (Klumperman et al., 1998).

The view that ERGIC clusters are transport vehicles rather than stable entities is largely based on studies where transport of GFP-labeled vesicular stomatitis virus G protein (VSV-G-GFP) through the secretory pathway was visualized in living cells (Presley et al., 1997; Scales et al., 1997; Lippincott-Schwartz et al., 2000). Upon ER exit, VSV-G-GFP becomes concentrated into bright fluorescent dots, localized adjacent to ERES that rapidly move to the Golgi area in a microtubule-dependent manner. Nevertheless, nothing in this data set precludes the possibility that the VSV-G-containing transport complexes, despite their considerable size and complexity, originate from a stationary ERGIC compartment by a dissociative process. By recording anterograde cargo only, a stationary ERGIC may not become apparent. What is needed, therefore, is the visualization of anterograde and retrograde traffic from the ERGIC. If the ERGIC clusters are just maturing transport carriers, anterograde and retrograde sorting would be expected to consume them. In the opposite scenario, the sorting event would leave behind ERGIC structures that persist, at least for a certain period, and are capable of multiple rounds of sorting.

In this report, we have visualized and quantified in living cells the trafficking of the recycling marker ERGIC-53 tagged with green fluorescent protein (GFP-ERGIC-53) and compared it with that of the well established anterograde reporter protein VSV-G-GFP and of a soluble secretory version of DsRed. We found GFP-ERGIC-53 in two distinct structures, long-lived and short-lived. The long-lived structures, corresponding to the previously described tubulovesicular clusters, are localized close to ERES, move little, and can undergo multiple rounds

of anterograde and retrograde sorting as well as cleavage and fusion. The short-lived structures are highly dynamic, move in all directions without preference for the Golgi area and are proposed to connect the stationary elements. These observations support the notion of a stationary ERGIC that is highly active in anterograde/retrograde sorting and can exchange material laterally.

Materials and Methods

Recombinant DNAs

Standard molecular biology protocols including PCR-based splicing and mutagenesis were used. Oligonucleotides were from Microsynth (Switzerland) and enzymes from New England BioLabs. GFP-ERGIC-53 was constructed in three steps: (1) The first AUG in the GFP coding sequence of the pEGFP-C1 vector (Clontech Laboratories) was removed using the gene splicing by overlap extension procedure; (2) The prolactin signal sequence (PRL) was amplified from a pCB6 vector construct in which it is upstream of a HA tag, and *Nhe*I restriction sites were introduced. The resulting PCR product was inserted into either pDsRedT1-N1 vector (Bevis and Glick, 2002) or the modified pEGFP-C1 vector (from step 1); (3) GFP-ERGIC-53 was engineered from pBluescript SK-ERGIC-53 construct (Schindler et al., 1993). The original signal sequence of ERGIC-53 was replaced by an *Xma*I restriction site and the generated PCR product was inserted into the pEGFPC1 vector containing the pre-prolactin signal sequence. Throughout this manuscript, GFP refers to the enhanced version of GFP. VSV-G tsO45 C-terminally tagged with GFP (here termed VSV-G-GFP) was as described (Scales et al., 1997). All constructs were verified by sequencing.

Cell culture, pulse-chase and immunoprecipitation

HeLa cells (ATCC) were grown in DMEM supplemented with 10% fetal bovine serum, non-essential amino acids, fungizone, penicillin and streptomycin. Calcium phosphate precipitation or Fugene6 (Roche) was used for transient transfections unless stated otherwise. 24 hours later, the cells were processed for imaging or for stable transfection. HeLa stable cell lines were produced by selection for G418 resistance (0.6 mg/ml; Sigma-Aldrich). Single clones were screened for expression with or without sodium butyrate induction (10 mM). Results are from at least two independent clones. HeLa cells grown in 3.5 cm dishes were subjected to pulse-chase using [^{35}S]methionine, followed by immunoprecipitation with mAb G1/93 (Schweizer et al., 1988) or anti-GFP (Boehringer Mannheim, Germany).

Immunofluorescence microscopy

Cells were cultured in eight-well Lab-Tek glass chamber slides (Nalge Nunc International). Cells were fixed with 3% paraformaldehyde and permeabilized with 0.1% saponin or 0.2% Triton X-100, 10 mM glycine and 0.1% sodium azide in PBS (solution 1). Non-specific binding was blocked by a 10-minute incubation in solution 1 containing 0.3% BSA. Cells were then incubated with primary antibodies diluted in solution 1 followed by appropriate secondary antibodies for 45-90 minutes. After several washings, the cells were embedded in Mowiol 4-88 (Calbiochem) supplemented with 1.3 mg/ml DABCO (Sigma-Aldrich). The following antibodies were used: mAb G1/296 anti-CLIMP63 (Schweizer et al., 1993), mAb G1/221 anti-transferrin receptor (Vollenweider et al., 1998), mAb maD anti-β-COP (Pepperkok et al., 1993), anti-Sec31 (Shugrue et al., 1999) and anti-Sec13 (Tang et al., 1997). Primary antibodies were detected with affinity-purified Alexa® 565 either goat-anti-mouse or goat anti-rabbit (Molecular Probes). Images were obtained using a Leica TCS NT confocal laser-scanning microscope, a 63× 1.32 NA or a 100× 1.4 NA lens, a pinhole diameter of 1 Airy unit, and 488 nm laser excitation for GFP and 568 nm for Alexa® 565.

Live cell imaging

HeLa cells were cultured on 18 mm round glass coverslips and treated with sodium butyrate overnight followed by incubation without sodium butyrate for a few hours. They were then transferred to imaging medium 1 (Ham's F12 supplemented with 20 mM HEPES, pH 7.4) in a Ludin chamber (Life Imaging Services GmbH, Switzerland, www.lis.ch) and imaged with a ×63 1.4 NA Plan-Apochromat oil objective on a Zeiss Axiovert 135M microscope at 37°C. Images were taken with a CCD camera (SensiCam; PCO Computer Optics) using a filter wheel to switch between excitation and emission wavelengths. The excitation/emission combinations used were at 480/525 for GFP and 565/620 for DsRed (Chroma Technology). ImagePro® Plus software (Media Cybernetics®) was used for both recording and image processing, which essentially consisted of narrowing the look-up table range and using a High Gauss and sharpening filters. Image J from NIH Image was also used for image processing (http://rsb.info.nih.gov/nih-image/). Speeds and displacements were measured using a macro written in NIH Image by Jens Rietdorf (ALMF, EMBL, Heidelberg). Fast dual recording and 4D imaging was done at the Advanced Light Microscopy Facility (ALMF) EMBL, Heidelberg. The imaging medium was MEM without phenol red, supplemented with 30 mM HEPES, pH 7.4 and 0.5 g/l sodium bicarbonate. For the dual color fast time-lapse recording, a temperature-controlled Olympus TILL/Photonics® time-lapse microscope, equipped with an emission beam splitter (DualView, OpticalInsights) that splits the emitted light into two spectrally distinct channels was used. The sample was excited at 488 nm and the fluorescence signal was split into two channels using a dichroid mirror (centered around 560 nm) and two emission filters (BP530/30 and LP590) introduced into the emission beam splitter. A Perkin Elmer spinning disc confocal microscope (UltraVIEWRS) mounted on a Zeiss Axiovert 200 microscope was used for 4D image acquisition. Individual *z*-stacks at distinct time-points were acquired using a ×60 Plan Neofluar objective and subsequently projected for each time-point separately using a macro written in IDL by Timo Zimmerman (ALMF, EMBL, Heidelberg).

Transport blocks

Cells were incubated in HEPES-buffered medium (20 mM HEPES, pH 7.4). To reversibly block traffic in the ERGIC, cells were incubated in DMEM at 15/16°C for 2-3 hours then rewarmed to 37/32°C and imaged. To block ERGIC-53 in the ER, cells were incubated on the temperature-controlled microscope stage for 20 minutes in imaging medium 1 supplemented with 50-90 μM H89 (Calbiochem). The drug was removed by flushing with fresh medium 1 warmed to 37°C. Data for quantification of sorting in stationary GFP-ERGIC-53 structures was collected from six different cells (each corresponding to a separate experiment) imaged every 10 seconds during rewarming. Yellow structures were counted and the first event to take place was scored. To quantify sorting in fast-moving structures, cells were imaged every 0.2 second for 1 minute at different rewarming times. The RGB movies collected were extracted into green and red, and all fast-moving structures were scored in both channels separately. Their overlap was then assessed over time.

Quantification of directionality

HeLa stable cell lines were pretreated for 16 hours with sodium butyrate, which was removed 6 hours prior to imaging. The cells were infected with adenovirus carrying the ts045-VSV-G-GFP DNA as described (Scales et al., 1997) and recorded during recovery from a 15/16°C block using a temperature-controlled spinning disk confocal

microscope (ALMF, EMBL, Heidelberg, Germany). Protein transport was measured at different rewarming times in six cells expressing GFP-ERGIC-53 or VSV-G-GFP using a program written in IGOR Pro (Wavemetrics, Lake Oswego, OR). The program is based on gradient-based optical flow estimation (Nomura et al., 1991) that measures the speed and direction of moving objects in an image sequence. We scored directions towards a reference point in the Golgi apparatus. Velocity and intensity filters were used to eliminate the apparent vectors generated by noise in the image sequence. The direction corresponds to the angle between the moving direction and the reference point. The direction is 0° when the spot moves straight to the reference point and 180° or –180° when moving straight away from the reference point. Directions were categorized by angle intervals. Particles moving in the interval of –60° to 60° were designated 'towards', those moving in the interval –120° to 120° were designated 'away', and the remaining angle values (–60° to –120° and 60° to 120°) were designated 'non-directional'. The directionality was measured for no longer than 10 seconds because during this time interval movement of spots and tubules could be tracked pixel by pixel and the precise direction quantified. Increasing the analysis time resulted in a more complex movement with several spots and tubules intersecting making it impossible to track them. Protein mass flow rates in each direction were calculated by multiplying fluorescence intensity and speed. The flow rate is thus a measure of transported protein per unit of time. Statistical significance ($P \leq 0.05$) of the preference in a certain direction among these three categories was probed by Student's *t*-test.

Results

Features of GFP-ERGIC-53 and endogenous ERGIC-53 are indistinguishable

To visualize the ERGIC and retrograde traffic from the ERGIC

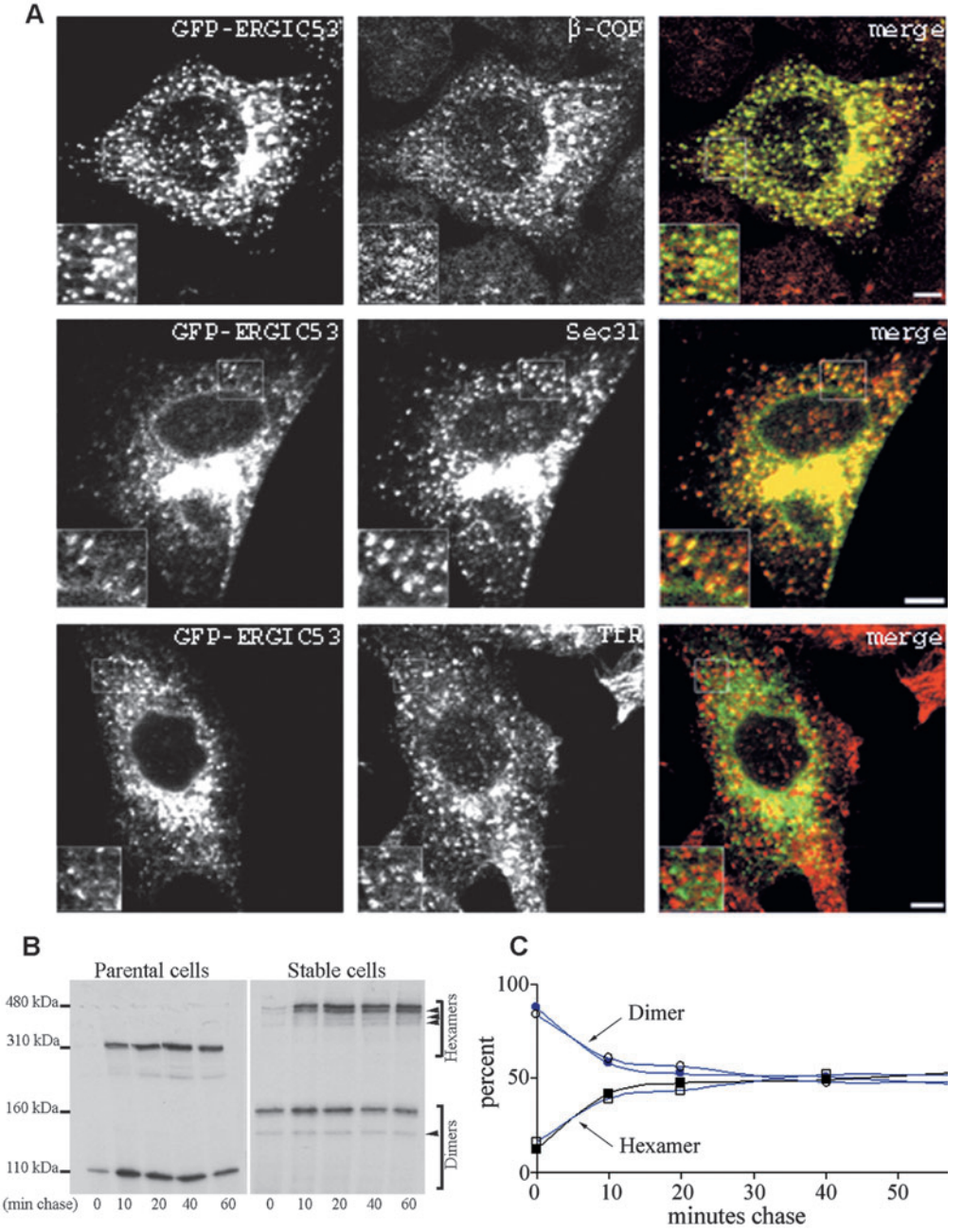

Fig. 1. GFP-ERGIC-53 localizes and oligomerizes like endogenous ERGIC-53. (A) HeLa cells stably expressing GFP-ERGIC-53 were treated with sodium butyrate overnight, fixed with paraformaldehyde, and stained for β-COP, Sec31 or transferrin receptor. Cells were observed with a confocal fluorescence microscope. Insets show higher magnifications. (B) GFP-ERGIC-53 cells treated with sodium butyrate or non-transfected cells were pulsed with [^{35}S]methionine and chased for the indicated times. Proteins were immunoprecipitated either with anti-ERGIC-53 for the control cells or with anti-GFP for the stable clone. Immunoprecipitates were analyzed by non-reducing SDS-PAGE and visualized by fluorography. During the time course, dimers (lower bands) disappear as hexamers (higher bands) form until a steady state is reached when each species is represented as 50%. GFP-ERGIC-53 dimers appear as two bands corresponding to homodimers and heterodimers (lower arrowhead) with endogenous ERGIC-53. These dimers are converted to hetero-hexamers (upper arrowheads) and homo-hexamers. (C) Quantification of dimer and hexamer formation during the chase period. 100% is the sum of homo-dimers and homo-hexamers at a given chase time. A representative experiment is shown. Bar, 5 μm.

in living cells we tagged ERGIC-53 with green fluorescent protein (GFP-ERGIC-53) and stably expressed it in HeLa cells. GFP was attached to the N-terminus of ERGIC-53 in order not to interfere with its trafficking, which is controlled by multiple position-dependent, C-terminal transport determinants (Kappeler et al., 1997; Nufer et al., 2002; Nufer et al., 2003). In some of the obtained clones GFP-ERGIC-53 was inducible by sodium butyrate, providing a means to study the effect of different expression levels of up to fourfold that of endogenous ERGIC-53. All the tested clones, however, gave similar results.

By confocal microscopy, GFP-ERGIC-53 localized to the Golgi area, peripheral dots and, less prominently, to the ER (Fig. 1A). This distribution is very similar to that of endogenous ERGIC-53 in non-transfected cells (supplementary material Fig. S1A). In the present work, we mainly focused on peripheral structures, as labeling in the Golgi area is too dense to distinguish individual ERGIC spots. Like endogenous ERGIC-53, GFP-ERGIC-53 colocalized with the COP I subunit β-COP and there was partial overlap with the distribution of the COP II subunit Sec31 (Fig. 1A) (Klumperman et al., 1998; Shima et al., 1999; Hammond and Glick, 2000). In transiently transfected COS cells highly overexpressing ERGIC-53, a fraction of the protein escapes to the plasma membrane and is subsequently endocytosed by a signal-mediated process (Hauri et al., 2000). This is not the case, however, in our HeLa clones expressing GFP-ERGIC-53, as no co-labeling with the endosomal marker transferrin receptor (Fig. 1A) or the lysosomal marker Lamp1 (data not shown) was observed.

To test if GFP-ERGIC-53 oligomerizes correctly into disulfide-linked dimers and hexamers (Schweizer et al., 1988), cells were metabolically labeled with [^{35}S]methionine in a pulse-chase experiment and ERGIC-53 was immunoprecipitated and analyzed by SDS-PAGE under non-reducing conditions. Fig. 1B shows that GFP-ERGIC-53 initially appears as a 160 kDa band corresponding to homodimers which is in part converted to a 480 kDa species corresponding to homohexamers. These high molecular weight species break down to an 80-kDa monomeric form under reducing conditions (data not shown). Importantly, the kinetics of conversion of dimeric to hexameric forms is identical to that of endogenous ERGIC-53 (Fig. 1C). Additional bands on the gel of GFP-ERGIC-53-expressing cells are hetero-oligomers formed between GFP-ERGIC-53 and the endogenous protein as these bands immunoprecipitated with both anti-GFP and anti-ERGIC-53 (supplementary material Fig. S1B). This hetero-oligomerization is an additional indication for correct folding of GFP-ERGIC-53.

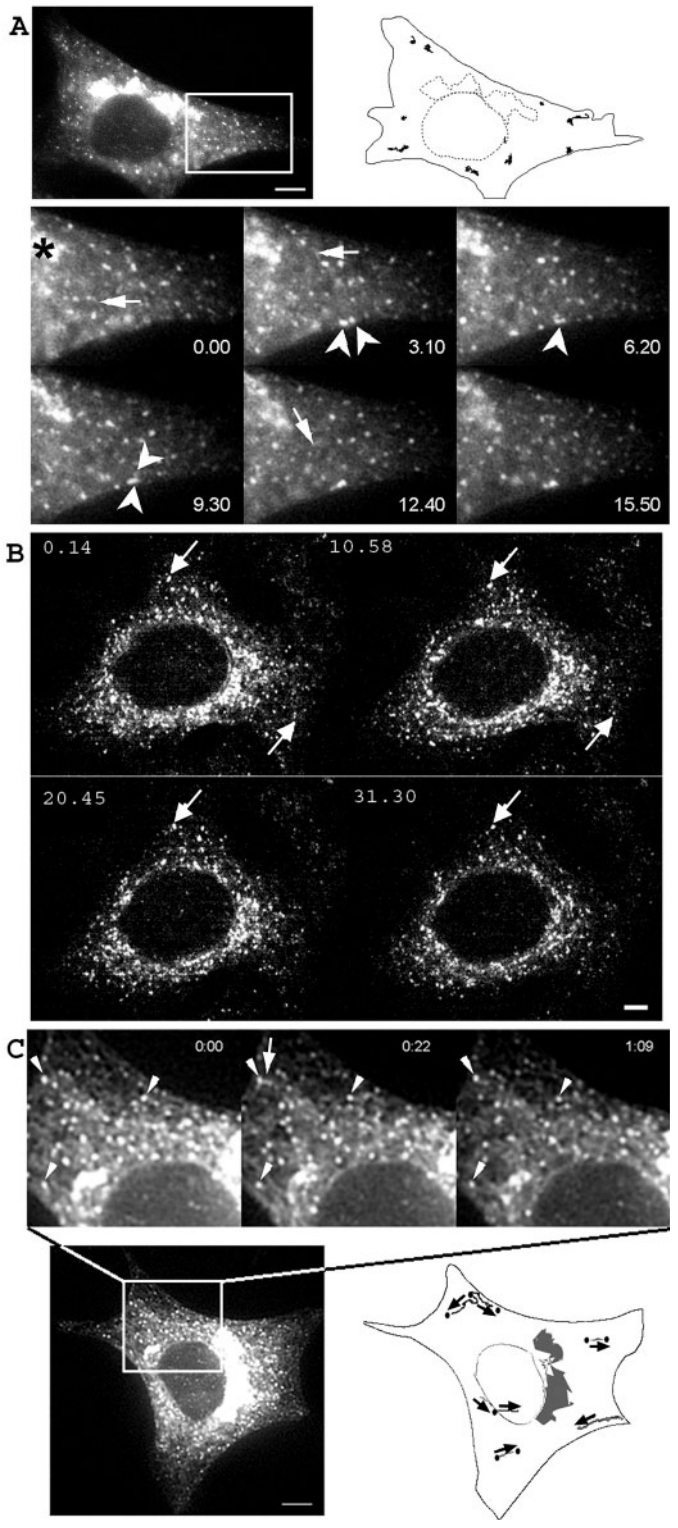

Fig. 2. Live imaging of GFP-ERGIC-53 reveals two types of structures with different dynamics. (A) A whole cell and its schematic representation where paths of stationary structures imaged every 10 seconds have been traced (see supplementary material Movie 2). Note that these structures undergo very short range to no movement. Lower panel shows image series of the outlined portion in the upper panel. Arrowheads point two peripheral ERGIC structures fusing with each other. Arrows indicate elongated ERGIC structures. (B) Representative images from supplementary material Movie 3. GFP-ERGIC-53-expressing HeLa cells were imaged in the *xyz* directions every 10 seconds. Arrows indicate long-lasting structures that can persist for up to 31 minutes. (C) Data taken from supplementary material Movie 4 imaged with an interval of 0.2 second. Representative frames show three peripheral ERGIC structures (arrowheads) that hardly move during the entire imaging interval. The arrow points to a peripheral stationary spot shooting out an elongated structure. Lower panel shows the whole cell and a schematic representation of paths that GFP-ERGIC-53 fast-moving structures followed during the imaging time. Note that the movement does not follow a defined direction, and often seems to connect two peripheral stationary structures. Bar, 5 μm. Time is shown as minutes.seconds.

Fluorescence recovery after photobleaching was then used to test if GFP-ERGIC-53 recycles. When the peripheral cytoplasm was bleached throughout the *z*-axis, fluorescent dots reappeared within 2 minutes (supplementary material Movie 1). We did not see non-bleached GFP-ERGIC-53 spots moving to refill the bleached area, suggesting that the reappearing dots largely originate from a recycling process involving the ER rather than a massive lateral transfer. The reappearance is not due to new protein synthesis as it also occurred in cycloheximide-treated cells. A similar recovery was observed when the Golgi area was bleached. Collectively, these data suggest that the GFP tag does not interfere with the folding and recycling of ERGIC-53.

GFP-ERGIC-53 imaging reveals two populations with different dynamics

To explore the dynamics of GFP-ERGIC-53 in living HeLa cells we used bright field and confocal time-lapse imaging with recording intervals of 10 seconds ('slow imaging') or 0.2 second ('fast imaging') to follow long- and short-time events, respectively.

Slow imaging of GFP-ERGIC-53 for 15 minutes (Fig. 2A) and longer (data not shown) revealed fluorescent puncta with a diameter of 0.9-1.2 μm exhibiting short-range movement of 1.2 μm on average with a maximal velocity of 0.2 μm/second (see supplementary material Movie 2). These structures did not move to the Golgi area but rather hovered about in place. We call them 'stationary' structures. They most probably correspond to the COP I-positive tubulovesicular clusters of the ERGIC previously identified by immunoelectron microscopy (Klumperman et al., 1998). Some stationary structures persisted throughout the entire recording time and occasionally fused with one another (Fig. 2A, arrowheads) or split. Others disappeared or appeared de novo in non-labeled areas. The fluorescence intensity of the spots did not remain constant but fluctuated with time indicating the continuous recycling of GFP-ERGIC-53. Recycling was confirmed by the recovery of fluorescence observed after partial bleaching of these spots (see arrows in supplementary material Movie 1). In rare cases, some dynamic tubular structures were observed that rapidly disappeared (Fig. 2A, arrows). They probably correspond to the fast-moving structures seen with fast imaging (see below).

To test if the appearance and disappearance of the stationary structures correspond to de novo formation and consumption events or to movement into or out of the focal plane, we performed 4D imaging (3D over time) using an imaging interval of 10 seconds and a step size of 0.8 μm. This approach showed that stationary GFP-ERGIC-53 spots can indeed form de novo or be consumed. Moreover, imaging for more than 30 minutes confirmed that many structures are long-lived, can undergo several fusion and splitting events, and do not exhibit a preferential movement to the Golgi area (Fig. 2B; supplementary material Movie 3). These features were

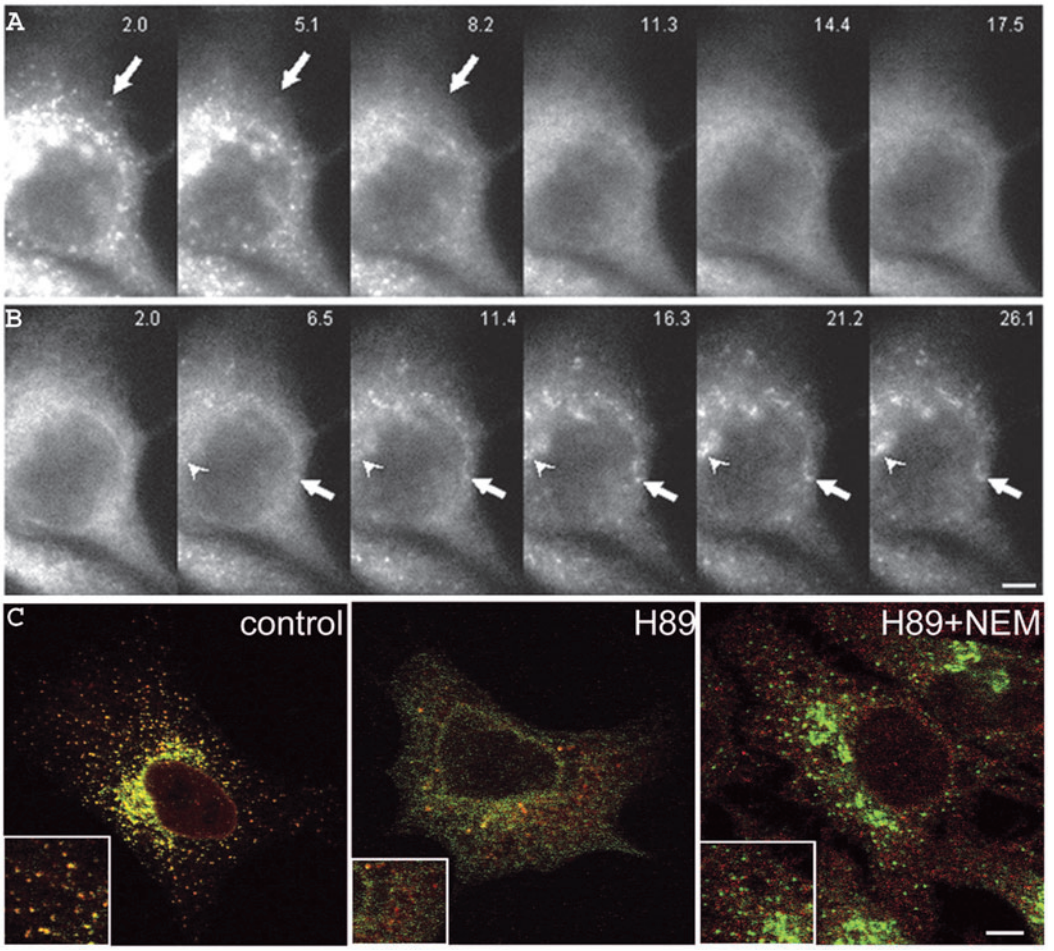

Fig. 3. ERGIC stationary structures in the periphery and in the Golgi area are equivalent. (A) Time points from supplementary material Movie 5 showing the relocalization of GFP-ERGIC-53 to the ER when cells are treated with H89. The arrow points to a peripheral ERGIC structure that loses fluorescence and disappears without moving to the Golgi area. (B) Time series from supplementary material Movie 6 showing the recovery of the same cell after H89 washout. The arrow points to a peripheral ERGIC structure that gets brighter during recovery but does not move to the Golgi area (arrowhead) which is refilled at the same time as peripheral ERGIC structures appear. (C) NEM blocks H89-induced recycling of GFP-ERGIC-53 to the ER. HeLa cells stably expressing GFP-ERGIC-53 were treated with H89 for 20 minutes in the presence or absence of NEM or left untreated (control), fixed with paraformaldehyde, stained for Sec13 (red), and analyzed by confocal microscopy. Insets show higher magnifications. Bar, 5 μm. Time is indicated as minutes.seconds.

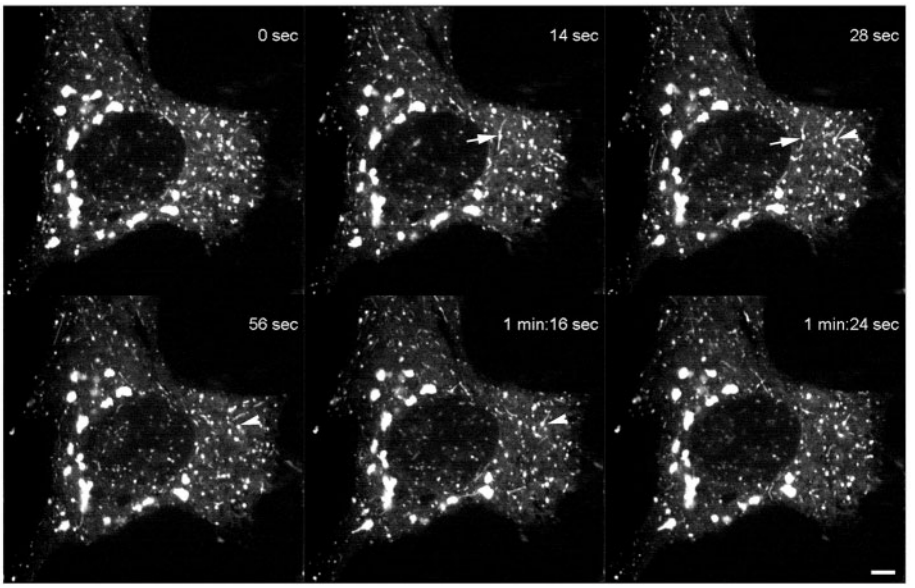

Fig. 4. GFP-ERGIC-53 tubule formation during rewarming from 16°C. GFP-ERGIC-53-expressing HeLa cells were incubated for 3 hours at 16°C, shifted to 37°C for 1 minute 53 seconds and imaged every 0.6 second (see supplementary material Movie 8). 0 second indicates the time at which imaging started. Extensive tubular structures appear from peripheral ERGIC spots and move with no preference in different directions. A single ERGIC structure can simultaneously extend tubules in opposite directions without being consumed (arrow). Several rounds of tubule emission from the same ERGIC spot do not consume it (arrowhead). Bar, 5 μm. Time, minutes.seconds.

unchanged when cells were imaged in the presence of cycloheximide to block protein synthesis.

Fast imaging (0.2-second intervals) of GFP-ERGIC-53 revealed, in addition to the stationary structures, short-lived fast-moving structures that were difficult to track under slow-imaging conditions. The short-lived elements moved in all directions and could occasionally be seen originating from stationary structures (supplementary material Movie 4; Fig. 2C). They had an apparent average diameter of 0.5 μm and moved in a stop-and-go fashion along curvilinear trajectories with speeds ranging from 1 to 7 μm/s. Often these structures seemed to cross each other, to move from one stationary structure to another or to cross several structures during their long-range movement of up to 6 μm. They frequently changed shape by becoming slightly elongated (supplementary material Movie 4). Tracking several of these structures for up to 70 seconds showed that they moved only rarely in the direction of the Golgi area (tracks in Fig. 2C). At 37°C, the fast-moving structures represented ~20% of all GFP-ERGIC-53 spots. Long tubules were infrequently seen. Their number was increased up to eightfold, however, when GFP-ERGIC-53 expression was induced by sodium butyrate treatment for 40 hours (data not shown). Fast movement was absent in cells preincubated on ice for 15 minutes and imaged at 37°C in the presence of nocodazole, suggesting microtubule dependence (data not shown). Collectively, our live-imaging approach revealed that most ERGIC-53 spots in the periphery are stationary and a minor population is highly dynamic.

Trafficking routes of GFP-ERGIC-53

To explore the dynamics of GFP-ERGIC-53 in more detail we used conditions that reversibly block protein recycling in the ER or ERGIC. Incubating the cells with the kinase inhibitor H89 known to block protein export from the ER (Aridor and Balch, 2000), relocalized GFP-ERGIC-53 to the ER (Fig. 3A; supplementary material Movie 5) as reported previously for endogenous ERGIC-53 (Lee and Linstedt, 2000). Antibody staining of fixed cells confirmed that during the H89 block, GFP-ERGIC-53 and endogenous ERGIC-53 increasingly colocalized with the ER marker CLIMP-63, whereas the structure of the Golgi defined by giantin remained unchanged (data not shown). Addition of H89 rapidly stopped the movement as well as the splitting and fusion activities of the peripheral stationary spots, and, synchronously with the Golgi area, the spots lost fluorescence within 20 minutes at the expense of an increasingly fluorescent ER (arrow in Fig. 3A; supplementary material Movie 5). H89 also stopped the fast moving structures (data not shown). Upon removal of H89, GFP-ERGIC-53 reappeared simultaneously in peripheral spots and the Golgi area (Fig. 3B; supplementary material Movies 6 and 7) whereas the ER fluorescence decreased concomitantly (compare Fig. 3B, recovery 2.0 and 26.1). Of note, the peripheral ERGIC structures did not directionally move to refill the Golgi area (arrow in Fig. 3B). This suggests that ERGIC structures in the periphery and in the Golgi area independently received GFP-ERGIC-53 from the ER. Fast-moving ERGIC-53 structures only appeared after almost full recovery of the stationary structures and often derived from them moving in all directions (data not shown).

To evaluate if the H89-induced redistribution of GFP-ERGIC-53 to the ER involves vesicular traffic we additionally included n-ethylmaleimide (NEM), which is known to block COP I vesicle fusion but not budding both in vitro and in vivo (Rothman and Orci, 1990). NEM prevented the retrograde traffic of GFP-ERGIC-53 to the ER although ER exit was blocked, as indicated by the diffuse appearance of the COPII component Sec13 (Fig. 3C). In the presence of NEM peripheral GFP-ERGIC-53 spots were slightly less abundant than in control cells presumably owing to uninhibited vesicular budding from ERGIC membranes. NEM did not alter the high mobility of GFP-ERGIC-53 trapped in the ER by H89 as monitored by FRAP (data not shown). These results are consistent with vesicular ERGIC to ER transport.

To study trafficking from the ERGIC, low temperature/rewarming experiments were performed. Incubation at 15-16°C is known to reversibly accumulate ERGIC-53 in the ERGIC (Lippincott-Schwartz et al., 1990; Schweizer et al., 1990; Klumperman et al., 1998). Upon rewarming from 16°C to 37°C, the stationary peripheral GFP-ERGIC-53 spots rapidly emitted tubules moving with an average velocity of around 1 μm/second (Fig. 4; supplementary material Movie 8), whereas the fast-moving structures had essentially the same

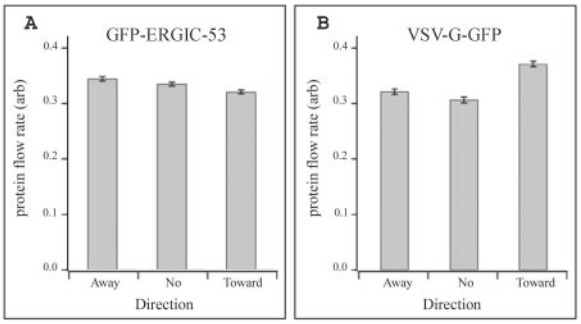

Fig. 5. GFP-ERGIC-53 and VSV G-GFP take different routes from the ERGIC. Quantification of the flow rate direction of GFP-ERGIC-53 (A) and VSV-G-GFP (B) in cells rewarmed from 16°C to 37°C or 15°C to 32°C, respectively. The protein flow rate is plotted in arbitrary units (normalized to 1) against the direction of movement. Note that VSV-G-GFP is directed toward the Golgi whereas GFP-ERGIC-53 is directed away from the Golgi. These differences are statistically significant (Student's *t*-test, $P \leq 0.05$). Bars show the mean±s.d. (GFP-ERGIC-53, $n=67$; VSV-G-GFP, $n=73$); No, non-directional movement.

movement as observed at 37°C (data not shown). Single stationary structures could repeatedly extend multiple tubules in different directions. The tubules formed and detached within seconds and stayed at peripheral sites for only brief periods before vanishing in the proximity of a stationary structure or disappearing in the cell periphery towards no defined structures. Formation and translocation of GFP-ERGIC-53-enriched tubules decreased with time until the activity entirely stopped 20 minutes after rewarming (data not shown). Tubule formation in general (81% of cases) did not consume the stationary structure. Moreover, the tubules had no apparent preference for moving to the Golgi area (Fig. 5).

To investigate whether these tubular processes were directed to the Golgi area, we photobleached this region in cells rewarmed from 16°C. At early recovery and rewarming times, tubules forming from peripheral spots extended randomly into different directions whereas the Golgi area was refilled homogeneously and independently of the tubules (data not shown). Obviously, the refilling of the Golgi area reflects direct transport of GFP-ERGIC-53 from the ER into ERGIC clusters that are concentrated near the Golgi apparatus and cannot be resolved by light microscopy (Klumperman et al., 1998). After 10 minutes of recovery, the profile of GFP-ERGIC-53-containing structures, including the Golgi area, was similar to that of the pre-bleached state. Collectively, these experiments suggest that the dynamic tubules indicate the ERGIC to ER recycling route and that the recycling of GFP-ERGIC-53 largely bypasses the Golgi.

GFP-ERGIC-53 and VSV-G-GFP take different routes from the ERGIC

Our conclusion regarding the recycling pathway of GFP-ERGIC-53 is based on visual analysis. To test this visual impression further, we sought to compare the traffic route of GFP-ERGIC-53 from the ERGIC quantitatively with that of the well-studied anterograde marker membrane protein VSV-G-GFP. To this end, we measured the directionality of protein flow rate after a low temperature block by a vector field method based on the optical flow estimation (see Materials and Methods). HeLa cells either stably expressing GFP-ERGIC-53 or infected with adenovirus carrying the ts045-VSV-G-GFP DNA were subjected to the low temperature/rewarming procedure and imaged at different rewarming times for approximately 100 seconds. We analyzed moving entities with speed ranges between 200 nm/second and 400 nm/second from several 10 seconds sub-sequences of each movie. There was enough displacement during this short period to measure directionality relative to the Golgi optimally. During rewarming from 16°C to 37°C, the movement of GFP-ERGIC-53 had a slight preference away from the Golgi (Fig. 5A). This is consistent with and quantitatively supports our visual impression that GFP-ERGIC-53 does not preferentially move to the Golgi. For VSV-G-GFP, rewarming from 15°C to 32°C generated a preferential movement toward the Golgi (Fig. 5B). This finding is in accord with previous reports on the dynamics of VSV-G-GFP during rewarming from 15°C (Presley et al., 1997; Scales et al., 1997). The seemingly small differences between towards and away unravel the particularities of VSV-G-GFP dynamics during exit from the ERGIC in a 15°C rewarming experiment. VSV-G-GFP exit from the ERGIC is gradual rather than a rapid switch. Simulations show that such small differences between towards and away produce a net directional transport of VSV-G to the Golgi as a result of cumulative effects. Collectively, these results show quantitatively that GFP-ERGIC-53 and VSV-G-GFP leave the ERGIC in different directions, consistent with their opposed transport to the ER and to the Golgi, respectively.

Sorting of anterograde and retrograde cargo in the ERGIC

To obtain sorting information also on a soluble secretory protein and to visualize the sorting of anterograde and retrograde cargo directly in the same cell we constructed a secretory form of pDsRedT1 (Bevis and Glick, 2002), termed ssDsRed, by attaching an N-terminal signal sequence. ssDsRed was transfected into HeLa cells stably expressing GFP-ERGIC-53 and transport was studied by dual color imaging.

Using immunoprecipitation experiments we verified that ssDsRed was indeed secreted into the culture medium (data not shown). When transport was blocked at 16°C, ssDsRed displayed an enhanced ER pattern, and some ERGIC-53 spots also co-labeled with ssDsRed. Rewarming to 37°C led to a gradual decrease of ER fluorescence followed by an increase in peripheral ERGIC structures and subsequently the Golgi area (Fig. 6A; supplementary material Movie 9). Large ssDsRed spots were clearly seen to leave the peripheral ERGIC spots. The number of exiting ssDsRed spots correlated with the expression level. We chose to analyze moderately expressing cells as they are closer to physiological conditions. To quantify ssDsRed segregation from peripheral ERGIC clusters we tracked structures colocalizing with GFP-ERGIC-53 in six cells and classified the different initial sorting events during rewarming from 16°C.

Table 1 shows that 55% of the stationary ERGIC structures efficiently sorted ssDsRed and ERGIC-53 in a single step, whereby ssDsRed structures of considerable size left the ERGIC and moved to the Golgi area while the GFP-ERGIC-53 spot remained stationary. In 12% of cases, the sorting was

incomplete. In 31% of the cases, no sorting was observed, but many of these elements underwent fission and fusion. In only 2% of the cases did the sorting result in complete consumption of the yellow ERGIC spot. Thus, in a majority of sorting events, the ERGIC remained stationary and was not consumed. Many of the ERGIC structures segregated ssDsRed repeatedly (Fig. 6A, empty arrowheads; supplementary material Movie 9) indicating anterograde flow through a persisting ERGIC structure. Importantly, the export of a ssDsRed dot often changed the color of the initial ERGIC cluster from yellow to more greenish in colour, suggesting that individual clusters act as entities in cargo sorting.

To make sure we did not miss fast sorting events we studied ssDsRed and GFP-ERGIC-53 segregation by the fast recording procedure. As with the slow recording, ssDsRed segregated from GFP-ERGIC-53 stationary structures (Fig. 6B, filled arrowheads). Of the fast moving structures, 29% were positive for both markers and therefore appeared yellow in merged images. When observed for up to 1 minute, 77% of these yellow structures showed no sign of sorting and often eventually fused with stationary structures indicating intra-ERGIC transport; 23% of the fast-moving yellow structures separated into a red and a green vehicle, which moved in opposite directions. Hence, some of the fast-moving structures exhibited bidirectional sorting.

Table 1. Quantification of GFP-ERGIC-53 and ssDsRed initial sorting in the ERGIC of live cells following rewarming from 15 to 37°C*

Observation	%	Consistent with stationary compartment model?
Complete sorting		
Export of ssDsRed spot, GFP-ERGIC-53 spot remains stationary	55	Yes
Consumption by sorting	2	No
Incomplete sorting		
Export of ssDsRed spot	7	Yes
Export of GFP-ERGIC-53 spot	5	Yes
No sorting	31	–

*Recordings were made at intervals of 10 seconds for 20 minutes (see Materials and Methods). % refers to total number of analyzed stationary ERGIC structures.

Discussion

Although no stable marker for the ERGIC is known, the continuous recycling of ERGIC-53 has allowed us to visualize the ERGIC for prolonged times in living cells and to compare the dynamics of sorting of the retrograde marker protein ERGIC-53 and the anterograde markers VSV-G and ssDsRed. Our findings shed new light on the nature of the ERGIC and on protein trafficking early in the secretory pathway. They support the notion of a stationary ERGIC consisting of numerous discontinuous elements that operate in bidirectional sorting to the ER and Golgi. This conclusion is based on three major observations. First, GFP-ERGIC-53 is localized in stationary spots displaying short-range non-directional movement. Unlike VSV-G-GFP spots, GFP-ERGIC-53 spots do not show a preferential movement toward the Golgi region and hence do not exhibit typical features of anterograde

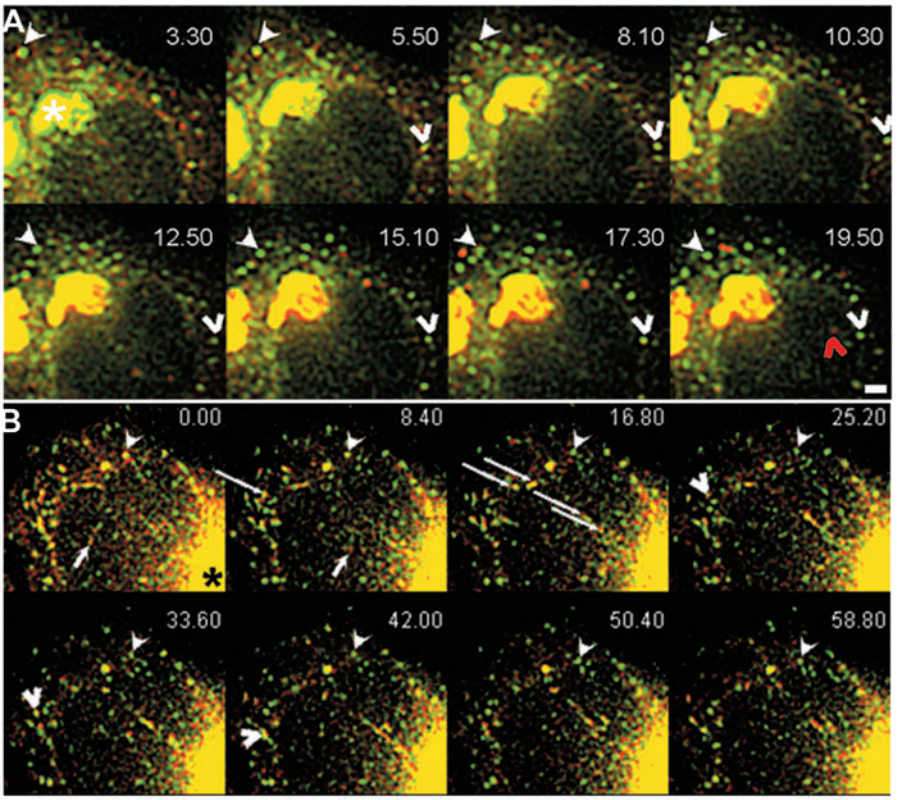

Fig. 6. Sorting of GFP-ERGIC-53 and ssDsRed in peripheral ERGIC structures. Data from cells co-expressing GFP-ERGIC-53 and ssDsRed rewarmed after a 3-hour 16°C block. (A) Time series (taken every 10 seconds) from supplementary material Movie 9. 3.30 indicates the time after rewarming to 37°C. The filled arrowhead indicates a stationary GFP-ERGIC-53 structure from which ssDsRed segregates. Note that even in the proximity of the Golgi, the ERGIC stationary structure does not move toward this area. The empty arrowhead indicates another stationary structure from which ssDsRed segregates. 11 minutes 50 seconds later, this same structure receives new ssDsRed material that is shot toward the Golgi at time point 19.50 (red arrowhead). Note that the Golgi (asterisk) becomes redder as the rewarming proceeds. Time, minutes.seconds. (B) Cell imaged with an interval of 0.2 second, 12 minutes after shifting the temperature from 15°C to 37°C. 0.00 indicates the time at which the imaging started. The filled arrowhead points to a stationary structure that segregates ssDsRed as in A. Some GFP-ERGIC-53 structures are positive for ssDsRed and move together towards (arrow) the Golgi (asterisk) or toward other ERGIC structures (empty arrowhead). Often, moving structures carrying both GFP-ERGIC-53 and ssDsRed cross several GFP-ERGIC-53 stationary structures (long arrows). Time, seconds.milliseconds. Bar, 5 μm.

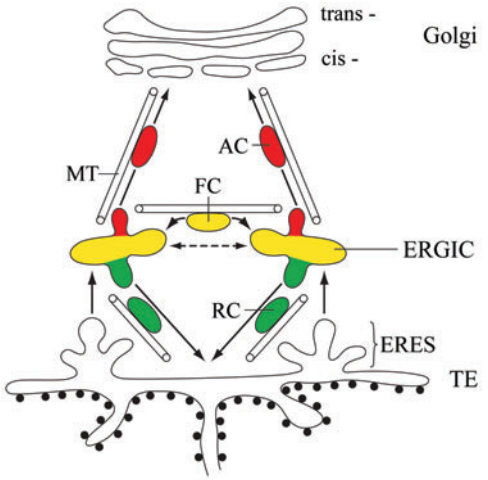

Fig. 7. Model of the organization of the early secretory pathway and sorting of anterograde and retrograde traffic in the ERGIC. The cycling protein GFP-ERGIC-53 (green) and anterograde cargo, such as VSV-G-GFP or ssDsRed (red), leave the ER at ER-exit sites (ERES) of the transitional elements of the rough ER (TE) and are transported to the ER-Golgi intermediate compartment (ERGIC) by a microtubule-independent process. The ERGIC is a collection of stationary tubulovesicular clusters exhibiting short range, non-directional, but microtubule-dependent movement. The clusters can split or fuse with one another (dashed arrow). Sorting in the ERGIC leads to anterograde carriers (AC), mediating transport of ssDsRed to the cis-Golgi and to retrograde carriers (RC) mediating transport of GFP-ERGIC-53 back to the ER. Both pathways are dependent on intact microtubules. Individual ERGIC-clusters are connected by fast-moving carriers (FC) that carry both markers and are transported along microtubules. MT, microtubules.

carriers (ACs). Their short-range movement is dependent on intact microtubules as it is lost in nocodazole-treated cells. Second, many of the stationary GFP-ERGIC-53 structures are long-lived and persist for more than 30 minutes, another feature that is inconsistent with an exclusive AC function. ER to Golgi transport is a rapid event. The ERGIC spots can undergo splitting and occasionally fuse with one another; some appear de novo, others disappear. Interestingly, similar features have been observed for ERES (Stephens, 2003; Bevis and Glick, 2002) suggesting that the dynamics of ERES and ERGIC clusters may be regulated in concert. Third, the ERGIC spots are not consumed by the sorting of GFP-ERGIC-53 and ssDsRed. They can undergo multiple rounds of sorting of anterograde and retrograde cargo.

Our conclusion regarding the nature of the ERGIC is different from previous live-imaging studies on VSV-G-GFP transport (Presley et al., 1997; Scales et al., 1997). These authors concluded that the ERGIC clusters are transport vehicles for protein delivery to the Golgi, rather than a stable compartment (Lippincott-Schwartz et al., 2000). In accord with these studies, we observed that the ACs moving to the Golgi, containing ssDsRed (or VSV-G-GFP), are rather large and cannot be small transport vesicles. However, they derive from the stationary ERGIC defined by ERGIC-53. Only by visualization of the sorting of anterograde and retrograde traffic from the ERGIC in living cells did the stationary nature of this compartment become apparent.

Quantification of the directionality of movement by a numerical processing procedure supports our visual impression that GFP-ERGIC-53 largely escapes packaging into ACs. Unlike VSV-G-GFP, GFP-ERGIC-53 shows no preferential movement to the Golgi upon exit from the ERGIC: it moves in the opposite direction. Considering the apparently random distribution of ERGIC clusters in the peripheral cytoplasm one would expect no preferred directionality for GFP-ERGIC-53 cycling back to the ER. However, low temperature blocks tend to concentrate the ERGIC clusters closer to the Golgi apparatus (Klumperman et al., 1998). Therefore, the measured net flow for ERGIC-53 results from a combined effect: repositioning of ERGIC clusters and recycling of ERGIC-53. At first glance, the measured difference of 13.5% between anterograde and retrograde movements of VSV-G-GFP appears to be small. It should be noted, however, that the quantification time was short (10 seconds) and that extrapolation to a longer time results in a net flow to the Golgi within a few minutes. Thus, directed transport is the consequence of a slight preference in movement towards one direction. Overall, this novel vector field method based on the optical flow estimation validates previous conclusions derived from fixed cells (Klumperman et al., 1998), proposing that ERGIC to ER retrograde transport largely bypasses the Golgi. It is also consistent with our ssDsRed/GFP-ERGIC-53 dual-imaging data showing preferential sorting of anterograde and retrograde traffic in the ERGIC.

ERGIC clusters defined by ERGIC-53 and COP I are localized in close proximity to ERES (Bannykh et al., 1996; Klumperman et al., 1998; Martinez-Menarguez et al., 1999; Stephens et al., 2000), which precludes the visualization of protein transport from ERES to ERGIC in live cells owing to the insufficient resolution of light microscopy. Therefore, a simple alternative interpretation of our data would be that GFP-ERGIC-53, unlike endogenous ERGIC-53, is trapped in ERES and has no access to the ERGIC. Accordingly, the dispersal of GFP-ERGIC-53 induced by H89 could reflect diffusion within the plane of the ER membrane. Several observations argue against this interpretation. Like endogenous ERGIC-53, GFP-ERGIC-53 co-localizes with the COP I subunit β-COP but shows only partial overlap with COPII subunits, Sec13 and Sec31, in fixed cells analyzed by confocal microscopy. Likewise, our biochemical analysis indicates normal folding of GFP-ERGIC-53. Furthermore, NEM blocks the H89-induced dispersal of ERGIC-53 from the stationary structures indicating discontinuity with the ERES. The combined data suggest that the GFP-ERGIC-53 stationary structures correspond to the tubulovesicular ERGIC clusters defined by ERGIC-53 and COP I at the ultrastructural level (Schweizer et al., 1988; Klumperman et al., 1998).

By imaging at high temporal resolution of 5 frames per second (fast imaging) we have uncovered a third pathway not previously described. This pathway is mediated by fast-moving carriers (FCs) a fraction of which contains both GFP-ERGIC-53 and ssDsRed. The pathway is highly sensitive to microtubule-disrupting drugs as well as H89, and requires the existence of stationary ERGIC structures as unveiled by H89 wash-out experiments. As FCs do not exhibit preferential movement to the Golgi area and can occasionally be seen to originate from and fuse with stationary ERGIC structures, we propose that they functionally connect ERGIC clusters by

lateral exchange. Although a majority of the FCs remains unsorted and appears to eventually fuse with a stationary structure, some can separate into a GFP-ERGIC-53-containing and an ssDsRed-containing dot, which move in opposite directions. The GFP-ERGIC-53 dot tends to rapidly disappear, whereas the ssDsRed dot moves to the Golgi. This suggests that some FCs are involved in anterograde/retrograde sorting.

Integrating our new data with previously published findings, the following picture regarding the organization and traffic routes in the early secretory pathway emerges (Fig. 7). Newly synthesized secretory proteins and ERGIC-53 are transported from the ER to stationary ERGIC clusters that are lying close to, but separate from ERES (Bannykh et al., 1996; Mezzacasa and Helenius, 2002). Although there is agreement that ER exit is COP II-dependent (Horstmann et al., 2002; Mironov et al., 2003), the precise mechanism of membrane traffic from ERES to ERGIC remains to be elucidated. Once in the ERGIC, anterograde cargo is sorted from ERGIC-53 into rather large ACs by a dissociative process. The size of ACs may vary according to cargo flux and can be considerable under conditions of massive synchronized release of VSV-G from the ER (Horstmann et al., 2002). ACs then rapidly move to the Golgi in a microtubule-dependent way. In contrast, ERGIC-53 is packaged into retrograde carriers (RCs), the size and shape of which can also vary. RCs must also be of a considerable size to be visible. When traffic is inhibited at 15°C followed by rewarming to 37°C, RCs emanating from the ERGIC clusters are often tubular. It appears that conditions of massive cargo transport favor the formation of tubules regardless of the pathway. Like ERGIC to Golgi anterograde transport, efficient ERGIC to ER retrograde transport requires intact microtubules.

What is the role of the newly discovered FCs that connect individual stationary ERGIC elements and are only visible at high temporal resolution? FCs may functionally link the ERGIC clusters allowing the exchange of critical components within the discontinuous ERGIC system. Alternatively, FCs may be incompletely sorted ACs that, because of their incomplete sorting, are unable to travel to the Golgi. Thereby, the FC pathway would operate as a backup system in order to prevent anterograde transport of incompletely sorted membranes.

Our study does not lend support to the notion of an ERGIC-53-positive late subdomain of ERGIC close to the Golgi as proposed by Marra and colleagues (Marra et al., 2001). Inconsistent with such a view, ERGIC-53 appears with indistinguishable kinetics in clusters close to the Golgi and in the periphery after H89 wash-out, and ACs moving from stationary ERGIC spots to the Golgi do not comprise detectable levels of ERGIC-53. Moreover, GFP-ERGIC-53 spots in the periphery and in the Golgi region are GM-130-negative in these cells (data not shown). Our data rather suggest that all ERGIC clusters are qualitatively very similar or identical.

In conclusion, we find that in living cells the ERGIC defined by ERGIC-53 is composed of stationary long-lived structures close to ERES. The ERGIC structures are sites of active sorting of anterograde and retrograde cargo. Both anterograde and retrograde transport from the ERGIC must involve a dissociative process, the precise molecular mechanism of which remains to be uncovered. In view of the new finding that the ERGIC is stationary, it is likely to have additional functions that remain to be uncovered.

We thank Beat Ludin, Jens Rietdorf and Timo Zimmermann for imaging assistance; Benjamin Glick for providing pDsRedT1; Fred Gorelick and Wanjin Hong for providing antibodies to Sec31 and Sec13; Käthy Bucher, Maria Susanna Balda and Karl Matter for continuous support; and the members of the Hauri and Pepperkok groups for suggestions. The study was supported by the Swiss National Science Foundation (H.-P.H.), the University of Basel (H.-P.H.) and a Quality of Life EU NetworkGrant QCRI-CT-2002-01272 (R.P.)

References

Aridor, M. and Balch, W. E. (2000). Kinase signaling initiates coat complex II (COPII) recruitment and export from the mammalian endoplasmic reticulum. *J. Biol. Chem.* **275**, 35673-35676.

Aridor, M., Bannykh, S. I., Rowe, T. and Balch, W. E. (1995). Sequential coupling between COPII and COPI vesicle coats in endoplasmic reticulum to Golgi transport. *J. Cell Biol.* **131**, 875-893.

Bannykh, S. I. and Balch, W. E. (1997). Membrane dynamics at the endoplasmic reticulum-Golgi interface. *J. Cell Biol.* **138**, 1-4.

Bannykh, S. I., Rowe, T. and Balch, W. E. (1996). The organization of endoplasmic reticulum export complexes. *J. Cell Biol.* **135**, 19-35.

Bevis, B. J. and Glick, B. S. (2002). Rapidly maturing variants of the Discosoma red fluorescent protein (DsRed). *Nat. Biotechnol.* **20**, 83-87.

Beznoussenko, G. V. and Mironov, A. A. (2002). Models of intracellular transport and evolution of the Golgi complex. *Anat. Rec.* **268**, 226-238.

Blum, R., Stephens, D. J. and Schulz, I. (2000). Lumenal targeted GFP, used as a marker of soluble cargo, visualises rapid ERGIC to Golgi traffic by a tubulo-vesicular network. *J. Cell Sci.* **113**, 3151-3159.

Farquhar, M. G. (1985). Progress in unraveling pathways of Golgi traffic. *Annu. Rev. Cell Biol.* **1**, 447-488.

Glick, B. S. and Malhotra, V. (1998). The curious status of the Golgi apparatus. *Cell* **95**, 883-889.

Hammond, A. T. and Glick, B. S. (2000). Dynamics of transitional endoplasmic reticulum sites in vertebrate cells. *Mol. Biol. Cell* **11**, 3013-3030.

Hauri, H. P., Kappeler, F., Andersson, H. and Appenzeller, C. (2000). ERGIC-53 and traffic in the secretory pathway. *J. Cell Sci.* **113**, 587-596.

Horstmann, H., Ng, C. P., Tang, B. L. and Hong, W. (2002). Ultrastructural characterization of endoplasmic reticulum – Golgi transport containers (EGTC). *J. Cell Sci.* **115**, 4263-4273.

Kappeler, F., Klopfenstein, D. R., Foguet, M., Paccaud, J. P. and Hauri, H. P. (1997). The recycling of ERGIC-53 in the early secretory pathway. ERGIC-53 carries a cytosolic endoplasmic reticulum-exit determinant interacting with COPII. *J. Biol. Chem.* **272**, 31801-31808.

Klumperman, J., Schweizer, A., Clausen, H., Tang, B. L., Hong, W., Oorschot, V. and Hauri, H. P. (1998). The recycling pathway of protein ERGIC-53 and dynamics of the ER-Golgi intermediate compartment. *J. Cell Sci.* **111**, 3411-3425.

Lee, T. H. and Linstedt, A. D. (2000). Potential role for protein kinases in regulation of bidirectional endoplasmic reticulum-to-Golgi transport revealed by protein kinase inhibitor H89. *Mol. Biol. Cell* **11**, 2577-2590.

Lippincott-Schwartz, J., Donaldson, J. G., Schweitzer, A., Berger, E. G., Hauri, H.-P., Yuan, L. C. and Klausner, R. D. (1990). Microtubule-dependent retrograde transport of proteins into the ER in the presence of brefeldin A suggests an ER recycling pathway. *Cell* **60**, 821-836.

Lippincott-Schwartz, J., Roberts, T. H. and Hirschberg, K. (2000). Secretory protein trafficking and organelle dynamics in living cells. *Annu. Rev. Cell Dev. Biol.* **16**, 557-589.

Lotti, L. V., Torrisi, M. R., Pascale, M. C. and Bonatti, S. (1992). Immunocytochemical analysis of the transfer of vesicular stomatitis virus G glycoprotein from the intermediate compartment to the Golgi complex. *J. Cell Biol.* **118**, 43-50.

Marra, P., Maffucci, T., Daniele, T., Tullio, G. D., Ikehara, Y., Chan, E. K., Luini, A., Beznoussenko, G., Mironov, A. and de Matteis, M. A. (2001). The GM130 and GRASP65 Golgi proteins cycle through and define a subdomain of the intermediate compartment. *Nat. Cell Biol.* **3**, 1101-1113.

Martinez-Menarguez, J. A., Geuze, H. J., Slot, J. W. and Klumperman, J. (1999). Vesicular tubular clusters between the ER and Golgi mediate

concentration of soluble secretory proteins by exclusion from COPI-coated vesicles. *Cell* **98**, 81-90.

Mezzacasa, A. and Helenius, A. (2002). The transitional ER defines a boundary for quality control in the secretion of tsO45 VSV glycoprotein. *Traffic* **3**, 833-849.

Mironov, A. A., Mironov, A. A., Jr, Beznoussenko, G. V., Trucco, A., Lupetti, P., Smith, J. D., Geerts, W. J., Koster, A. J., Burger, K. N., Martone, M. E. et al. (2003). ER-to-Golgi carriers arise through direct en bloc protrusion and multistage maturation of specialized ER exit domains. *Dev. Cell* **5**, 583-594.

Nomura, A., Miike, H. and Koga, K. (1991). Field theory approach for determining optical flow. *Pattern Recog. Lett.* **12**, 183-190.

Nufer, O., Guldbrandsen, S., Degen, M., Kappeler, F., Paccaud, J. P., Tani, K. and Hauri, H. P. (2002). Role of cytoplasmic C-terminal amino acids of membrane proteins in ER export. *J. Cell Sci.* **115**, 619-628.

Nufer, O., Kappeler, F., Guldbrandsen, S. and Hauri, H. P. (2003). ER export of ERGIC-53 is controlled by cooperation of targeting determinants in all three of its domains. *J. Cell Sci.* **116**, 4429-4440.

Palade, G. (1975). Intracellular aspects of the process of protein synthesis. *Science* **189**, 347-358.

Pelham, H. R. (1989). Control of protein exit from the endoplasmic reticulum. *Annu. Rev. Cell Biol.* **5**, 1-23.

Pepperkok, R., Scheel, J., Horstmann, H., Hauri, H. P., Griffiths, G. and Kreis, T. E. (1993). Beta-COP is essential for biosynthetic membrane transport from the endoplasmic reticulum to the Golgi complex in vivo. *Cell* **74**, 71-82.

Presley, J. F., Cole, N. B., Schroer, T. A., Hirschberg, K., Zaal, K. J. and Lippincott-Schwartz, J. (1997). ER-to-Golgi transport visualized in living cells. *Nature* **389**, 81-85.

Rothman, J. E. and Orci, L. (1990). Movement of proteins through the Golgi stack: a molecular dissection of vesicular transport. *FASEB. J.* **4**, 1460-1468.

Scales, S. J., Pepperkok, R. and Kreis, T. E. (1997). Visualization of ER-to-Golgi transport in living cells reveals a sequential mode of action for COPII and COPI. *Cell* **90**, 1137-1148.

Schekman, R. and Orci, L. (1996). Coat proteins and vesicle budding. *Science* **271**, 1526-1533.

Schindler, R., Itin, C., Zerial, M., Lottspeich, F. and Hauri, H. P. (1993). ERGIC-53, a membrane protein of the ER-Golgi intermediate compartment, carries an ER retention motif. *Eur. J. Cell Biol.* **61**, 1-9.

Schweizer, A., Fransen, J. A. M., Baechi, T., Ginsel, L. and Hauri, H.-P. (1988). Identification, by a monoclonal antibody, of a 53-kD protein associated with a tubular-vesicular compartment at the *cis*-side of the Golgi apparatus. *J. Cell Biol.* **107**, 1643-1653.

Schweizer, A., Fransen, J. A. M., Matter, K., Kreis, T. E., Ginsel, L. and Hauri, H.-P. (1990). Identification of an intermediate compartment involved in protein transport from ER to Golgi apparatus. *Eur. J. Cell Biol.* **53**, 185-196.

Schweizer, A., Ericsson, M., Bachi, T., Griffiths, G. and Hauri, H. P. (1993). Characterization of a novel 63 kDa membrane protein. Implications for the organization of the ER-to-Golgi pathway. *J. Cell Sci.* **104**, 671-683.

Shima, D. T., Scales, S. J., Kreis, T. E. and Pepperkok, R. (1999). Segregation of COPI-rich and anterograde-cargo-rich domains in endoplasmic-reticulum-to-Golgi transport complexes. *Curr. Biol.* **9**, 821-824.

Shugrue, C. A., Kolen, E. R., Peters, H., Czernik, A., Kaiser, C., Matovcik, L., Hubbard, A. L. and Gorelick, F. (1999). Identification of the putative mammalian orthologue of Sec31P, a component of the COPII coat. *J. Cell Sci.* **112**, 4547-4556.

Stephens, D. J. (2003). De novo formation, fusion and fission of mammalian COPII-coated endoplasmic reticulum exit sites. *EMBO Rep.* **4**, 210-217.

Stephens, D. J. and Pepperkok, R. (2001). Illuminating the secretory pathway: when do we need vesicles? *J. Cell Sci.* **114**, 1053-1059.

Stephens, D. J., Lin-Marq, N., Pagano, A., Pepperkok, R. and Paccaud, J. P. (2000). COPI-coated ER-to-Golgi transport complexes segregate from COPII in close proximity to ER exit sites. *J. Cell Sci.* **113**, 2177-2185.

Storrie, B. and Nilsson, T. (2002). The Golgi apparatus: balancing new with old. *Traffic* **3**, 521-529.

Tang, B. L., Low, S. H., Hauri, H. P. and Hong, W. (1995). Segregation of ERGIC53 and the mammalian KDEL receptor upon exit from the 15 degrees C compartment. *Eur. J. Cell Biol.* **68**, 398-410.

Tang, B. L., Peter, F., Krijnse-Locker, J., Low, S. H., Griffiths, G. and Hong, W. (1997). The mammalian homolog of yeast Sec13p is enriched in the intermediate compartment and is essential for protein transport from the endoplasmic reticulum to the Golgi apparatus. *Mol. Cell. Biol.* **17**, 256-266.

Vollenweider, F., Kappeler, F., Itin, C. and Hauri, H. P. (1998). Mistargeting of the lectin ERGIC-53 to the endoplasmic reticulum of HeLa cells impairs the secretion of a lysosomal enzyme. *J. Cell Biol.* **142**, 377-389.

Journal of Cell Science